Journal of Nuclear Materials 407 (2010) 228–231

Contents lists available at ScienceDirect

Journal of Nuclear Materials

journal homepage: www.elsevier.com/locate/jnucmat

Letter to the Editor

Lanthanides migration in U–Zr based nuclear fuels

G. Bozzolo [a,*], H.O. Mosca [b], A.M. Yacout [a], G.L. Hofman [a]

[a] Argonne National Laboratory, 9700 S. Cass Av. Argonne, IL 60439, USA
[b] Gerencia de Investigaciones y Aplicaciones, CNEA, Av. Gral Paz 1499, B165KNA, San Martín, Buenos Aires, Argentina

ARTICLE INFO

Article history:
Received 23 August 2010
Accepted 5 October 2010

ABSTRACT

Atomistic modeling using the BFS method for alloys is performed to study the formation of lanthanide-rich precipitates in U–Zr fuel and the segregation patterns of all constituents to the surface. Surface energies for all elements were computed and, together with the underlying concepts of the BFS method, the migration of lanthanides to the surface region in U–Zr fuels is explained.

Lanthanides (LA) accumulate as fission products in metallic fuels and display strong migration patterns to the fuel surface reacting with cladding elements. Experiments show that lanthanides form distinct phases on the cladding inner surfaces or the periphery of the U–Zr based fuel. The fact that this occurs in fuel elements irradiated to only a few percent burnup suggests that the mechanism of transport is a rapid one. A model based on vapor phase transport has been proposed to explain this effect, by which lanthanides migrate, even at very low burnup, through a network of interconnected porosity which plays the role of a pathway to the surface [1]. Although this model has shown some level of success in explaining the observed behavior, it does not account for the quantity of these elements near or at the fuel cladding interface.

A quick examination of the phase diagrams of U-LA and Zr-LA provides a rationale for the formation of the observed LA-rich phases [2], but it does not account for the migration to the surface or the specific details distinguishing each LA (i.e., substantially preferred migration of Ce and its resulting strong interaction with cladding). No other explanation is currently available to explain the formation of LA-rich phases near the fuel surface or their migration pattern to the periphery.

With the purpose of investigating the behavior of LA in U–Zr based fuels, in this communication we report the results of an atomistic modeling approach based on a quantum approximate method for the energetics, namely, the Bozzolo–Ferrante–Smith (BFS) method for alloys [3]. The necessary parameters needed to describe the individual elements, as well as the BFS perturbative parameters describing the interactions among all elements were obtained from first principles calculations using the Linearized Augmented Plane Wave method [4] and determined from standard BFS procedures [5]. Exploiting the ability of BFS to deal with multicomponent systems [5], Metropolis–Monte Carlo simulations of U–Zr fuels with several lanthanides were performed, concentrating on the simulated annealing of large computational cells based on a U-10 wt.% Zr fuel. The initial state of the simulation was set as a random mix of all participating elements (U, Zr, Ce, Pr, Nd, Pm and Sm) and the cell was then treated with a descending temperature cycle. Different LA concentrations were tested keeping the overall percentage of LA below 10 at% for all participating elements (above the typical LA yield in normal operating conditions) but, within this range, little if any change in the outcome was found.

A representative example is the final low temperature state of a simulation of $U_{70}Zr_{20}Ce_2Pr_2Nd_2Pm_2Sm_2$, shown in Fig. 1, where the formation of several LA-based precipitates can be clearly seen. In addition to the randomly distributed initial cell, the $T = 900$ K and $T = 300$ K cells are shown. For this last case, detailed maps are shown for selected planes in the cell. This LA phase seems to induce the precipitation of a Zr phase with some Ce in solution, consistent with the solubility limit of Ce in Zr. The LA phase shows no particular ordering pattern of any kind, but some features can be extracted from the numerical analysis of the average coordination for each atomic species in the cell shown in Fig. 1. This is best seen in the short range order coordination matrix shown in Table 1, where the matrix element a_{AB} indicates the probability that an atom of species A has an atom B as a nearest-neighbor. Although the matrix is representative of the whole cell (i.e., it does not distinguish between the different phases seen in the cell), it can be seen that (1) Zr is as likely to bind to U atoms (U(Zr) solid solution) or create a Zr-rich environment, as a_{ZrU} and a_{ZrZr} are nearly identical, (2) Ce is the only element in solution in the Zr-rich phase, as expressed by a_{CeZr} being substantially larger than any a_{LAZr} matrix element, (3) the submatrix for lanthanides is perfectly symmetric, indicating that all LA can only be found in contact with each other (i.e., Ce has the same probability of having, for example, Pr as a nearest-neighbor as Pr has of having Ce), suggesting that the formation of different lanthanide precipitates with different compositions is purely a result of lanthanide diffusion in the fuel matrix, (4)

* Corresponding author. Tel.: +1 410 995 4063.
E-mail address: guille_bozzolo@yahoo.com (G. Bozzolo).

0022-3115/$ - see front matter © 2010 Elsevier B.V. All rights reserved.
doi:10.1016/j.jnucmat.2010.10.001

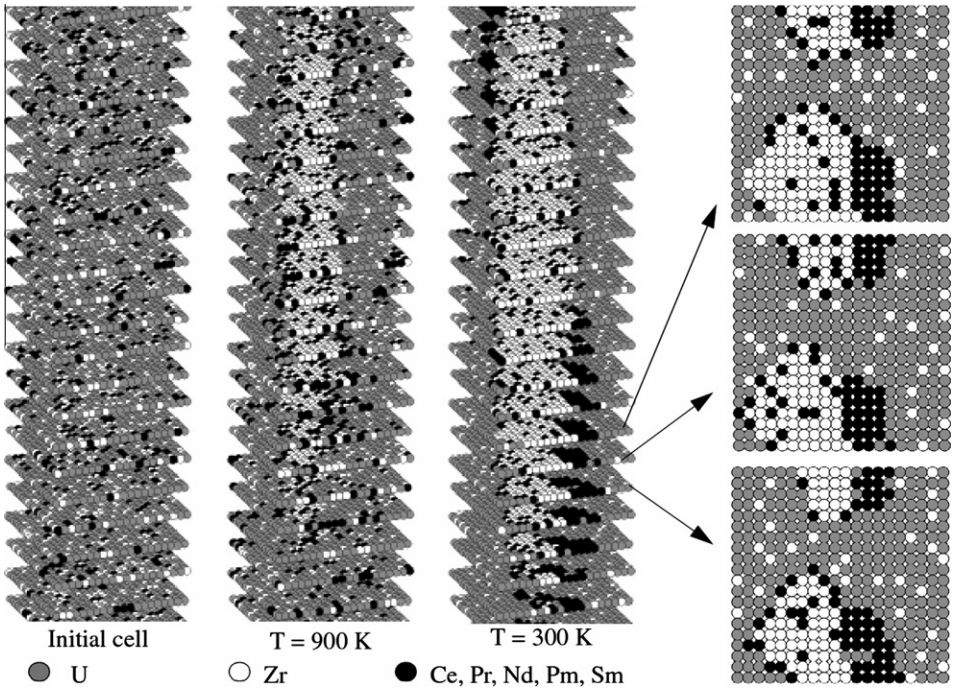

Fig. 1. Initial randomly distributed $U_{70}Zr_{20}Ce_2Pr_2Nd_2Pm_2Sm_2$ cell, and intermediate temperature states during simulated annealing. The last column shows detail of three consecutive planes in the $T = 300$ K equilibrium cell. U, Zr and LA atoms (LA = Ce, Pr, Nd, Pm and Sm) are denoted in grey, white and black.

the distribution of LA within the precipitates is not uniform, as indicated by the values of a_{LAU}, maximum for Nd, followed by Sm which, conversely, have the minimum values of a_{LAZr}, indicating their preferred contact with U-rich regions of the fuel, and (5) a wide range of LA grouping within the LA precipitates, maximum for Sm, indicated by the large diagonal elements of the LA submatrix (a_{LALA}).

The presence of a surface (whether a pore or the outer surface of the fuel) naturally changes the outcome of the simulations, now characterized by LA migration to it. To investigate this, simulations were performed adding a free surface in several crystallographic orientations. In this case, the initial state in the simulation consists of a bulk-terminated surface with an increasing temperature cycle (from room temperature up to $T = 1000$ K). Being that the fuel matrix has the bcc structure, the following results are restricted to the (1 1 0) surface, which has the lowest surface energy for bcc systems, thus guaranteeing the best approximation to a true polycrystalline surface. Representative results are shown in Fig. 2, where concentration profiles of intermediate states in the simulation are shown, corresponding to low ($T = 300$ K), intermediate ($T = 600$ K) and higher temperatures ($T = 1000$ K), the latter being a representative case of operating temperatures in the reactor.

Table 1
Coordination matrix for the final state of a simulation of $U_{70}Zr_{20}Ce_2Pr_2Nd_2Pm_2Sm_2$. Each entry represents the probability that an atom listed in the first column is nearest-neighbor with an atom in subsequent columns.

	U	Zr	Ce	Pr	Nd	Pm	Sm
U	84.91	12.02	0.09	0.69	1.06	0.46	0.78
Zr	42.06	44.88	8.46	1.43	0.95	1.04	1.17
Ce	3.20	84.61	0.78	3.24	3.32	2.73	2.11
Pr	24.06	14.34	3.24	17.19	11.05	16.91	13.20
Nd	37.11	9.53	3.32	11.05	8.05	18.28	12.66
Pm	16.05	10.39	2.73	16.91	18.28	24.61	11.02
Sm	27.15	11.68	2.11	13.2	12.66	11.02	22.19

The profiles show the concentration of each element in the surface (labeled zero), subsurface planes (labeled with positive numbers) and overlayers (labeled with negative numbers). Fig. 2a shows already the formation of subsurface LA-rich phases (increased LA concentration in subsurface planes, above their nominal bulk concentration), Zr depletion in the near-surface planes and LA migration to the surface plane (nearly equally shared by every possible LA). As the temperature increases, Zr segregates to the top subsurface planes. As shown in previous work using BFS for modeling of U–Zr surfaces [6], Zr enrichment of the surface region led by strain-driven segregation of Zr in low Zr concentration U–Zr alloys is seen, but as the temperature increases thermal effects create near-bulk conditions due to enhanced U presence in the surface. The migration of lanthanides to the surface is extremely strong, consistent with experimental observations of LA behavior in U–Zr based fuels [1,2]. This drives U and Zr concentration in the surface layers to lower values than otherwise possible. The simulation also shows three distinct regimes, illustrated by the concentration profiles shown in Fig. 2: (1) a low temperature regime characterized by strong Ce segregation to the surface layer than any other LA and depopulation of Zr in the subsurface, (2) an intermediate temperature regime with enhanced presence of Zr and all LA in the surface, and (3) a high temperature regime characterized by stronger Zr segregation to the subsurface layers. Enhanced LA surface concentration also leads to reconstruction of the surface, as can be seen in Fig. 3, where the top layers, corresponding to the example in Fig. 2c, are shown. The abundance of pits and terraces leads to incomplete (i.e., less than 100%) total planar concentration, as seen in the profiles in Fig. 2c.

Independently of the diffusion mechanism that might lead to LA surface segregation and surface composition, one reason that explains LA migration and the ensuing enhanced presence in the surface region is the surprisingly low surface energies of all LA with respect to U and Zr, as computed with BFS. Table 2 shows characteristic room-temperature surface energies for U, Zr, Ce, Pr, Nd, Pm and Sm for monatomic semi-infinite bcc cells with low Miller index

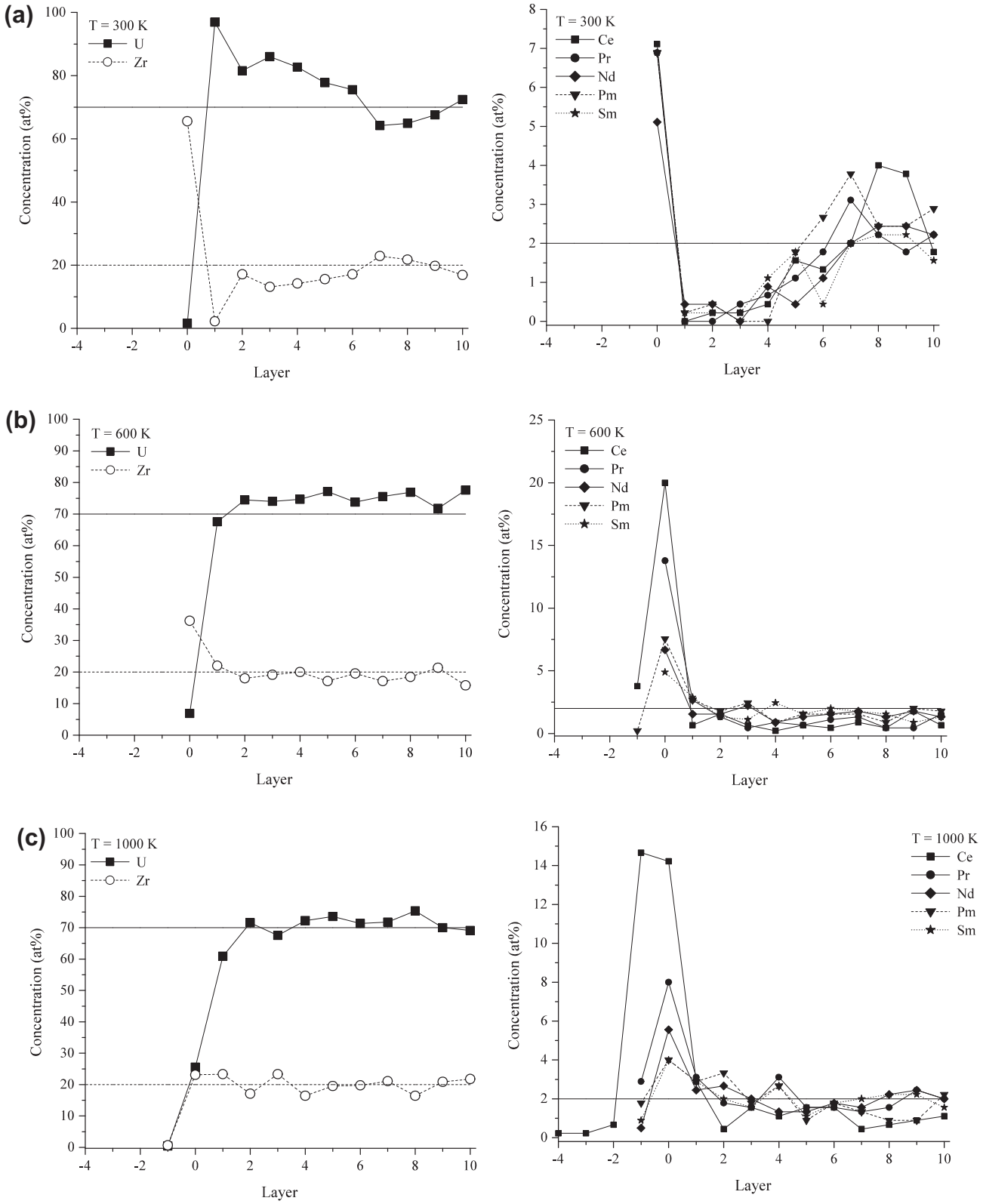

Fig. 2. Concentration profiles (in at%) for intermediate states of the slow heating simulation of a (1 1 0)-terminated $U_{70}Zr_{20}Ce_2Pr_2Nd_2Pm_2Sm_2$ computational cell for (a) T = 300 K, (b) T = 600 K, and (c) T = 1000 K. The horizontal lines represent the nominal concentrations for U (70 at%), Zr (20 at%), and each lanthanide (2 at%).

termination, computed with BFS. While the surface energy of U and Zr are rather similar, the surface energies of all LA are exceedingly low. This leads to dominant Ce segregation over any other element, followed by Pr and then, with minor differences, all the others. These results are also consistent with the observed strong interaction of Ce and other lanthanides with cladding (see Fig. 28 in Ref. [1]), which can only be due to their enhanced surface presence.

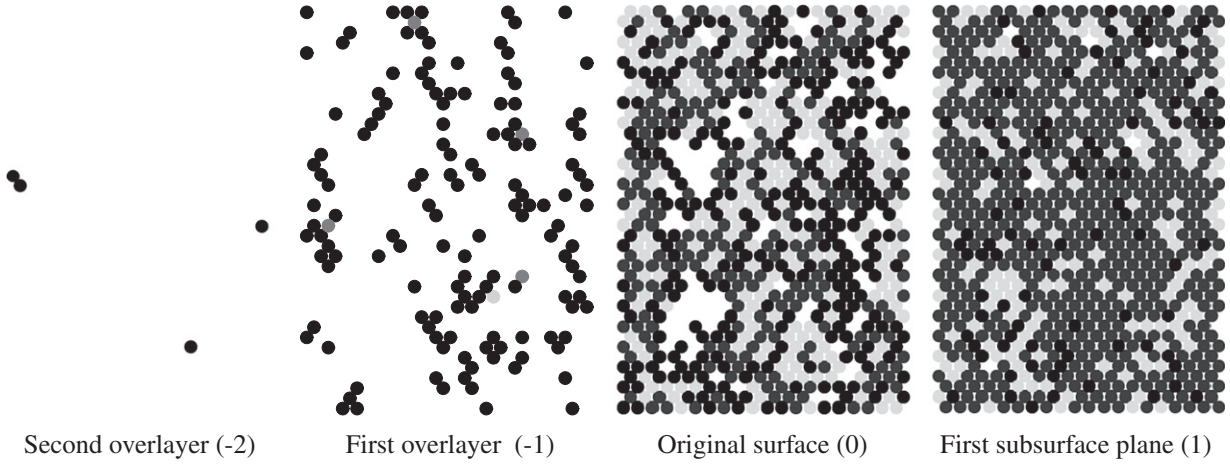

Fig. 3. Top view of the second overlayer (labeled –2 in Fig. 2), first overlayer (–1), original surface (0), and first plane below the surface (1) for the $T = 1000$ K case shown in Fig. 2c. U, Zr and LA atoms are shown in dark grey, light grey, and black circles, respectively. White areas in these maps denote empty sites. No distinction is made between the different LA. Details on LA plane concentration can be seen in Fig. 2c.

Table 2
Surface energies (in erg/cm^2) of U, Zr, Ce, Pr, Nd, Pm, and Sm for the (1 0 0), (1 1 0) and (1 1 1) orientations of the pure bcc crystals of each element.

	(1 0 0)	(1 1 0)	(1 1 1)
U	1906.30	856.06	1320.46
Zr	1924.06	866.75	1350.38
Ce	230.82	77.36	158.15
Pr	371.02	132.73	253.70
Nd	495.24	152.70	284.15
Pm	438.39	160.78	299.66
Sm	459.79	186.40	315.59

Acknowledgments

Fruitful discussions with N. Bozzolo are gratefully acknowledged. This work was supported under US Department of Energy Contract DE-AC02-06CH11357.

References

[1] G.L. Hofman, L.C. Walters, in: R.W. Cahn, P. Haasen, E.J. Kramer (Eds.), VCH Verlagsgesellschaft mbH (1994) 1.
[2] Y.S. Kim, G.L. Hofman, A.M. Yacout, J. Nucl. Mater. 392 (2009) 164–170.
[3] G. Bozzolo, J. Ferrante, J.R. Smith, Phys. Rev. B 45 (1992) 493.
[4] P. Blaha, K. Schwarz, G. K. H. Madsen, D. Kvasnicka and J. Luitz, WIEN2K, An Augmented Plane Wave + Local Orbitals Program for Calculating Crystal Properties (Karlheinz Schwarz, Techn. Universität Wien, Austria), 2001. ISBN 3-9501031-1-2.
[5] G. Bozzolo, H.O. Mosca, M.F. del Grosso, Intermetallics 16 (2008) 668.
[6] G. Bozzolo, H.O. Mosca, A.M. Yacout, G.L. Hofman, Y.S. Kim, Compos. Mater. Sci., doi:10.1016/j.commatsci.2010.09.002.